

Adsorption of Benzene, Fluorobenzene and Meta-di-Fluorobenzene on Cu(110): A Computational Study

L. A. ZOTTI,¹ G. TEOBALDI,¹ K. PALOTÁS,¹ W. JI,² H.-J. GAO,² W. A. HOFER¹

¹Surface Science Research Centre, University of Liverpool, L69 3BX Liverpool, United Kingdom

²Institute of Physics, Chinese Academy of Sciences, Beijing 100080, China

Received 16 October 2007; Revised 14 December 2007; Accepted 18 December 2007

DOI 10.1002/jcc.20916

Published online 21 February 2008 in Wiley InterScience (www.interscience.wiley.com).

Abstract: We modelled the adsorption of benzene, fluorobenzene and meta-di-fluorobenzene on Cu(110) by Density Functional Theory. We found that the adsorption configuration depends on the coverage. At high coverage, benzene assumes a tilted position, while at low coverage a horizontal slightly distorted geometry is favoured. Functionalizing the benzene ring with one or two fluorine atoms weakens the bonding to the surface. A rotation is induced, which decreases the distance of the fluorine atom from the surface. STM simulations reveal that details about both, benzene adsorption geometry and fluorine position, can be only detected at short tip-surface distances.

© Crown copyright 2008. J Comput Chem 29: 1589–1595, 2008

Key words: benzene; fluorobenzene; difluorobenzene; Cu(110); density functional theory; scanning tunneling microscopy

Introduction

The interaction of aromatic compounds with metals is of great interest: for instance, they can be connected to thiol molecules in the construction of molecular wires which can be exploited in building devices.¹ Benzene as the smallest aromatic molecule has been extensively studied as a model system for larger aromatic compounds. It is easily resolved in scanning tunneling microscopy (STM), because the delocalized π system of the aromatic ring gives a clear signature via its overlaps with states of the probe tip.² The adsorption of benzene on Cu(110) has been the object of several studies. Here, a critical issue is the orientation of the benzene ring with respect to the surface. Clarifying this point is important for molecular electronics, especially in single molecular junctions, where the molecular adsorption geometry plays a critical role.³

Lomas et al. stated⁴ that the molecular plane is substantially tilted with respect to the metal surface at both 2.4×10^{14} mol/cm² and 6.5×10^{14} mol/cm² coverages. This conclusion was drawn from angularly resolved photoemission spectra. It was visible by the presence at higher exit angles of some components, which are not found if the molecule is parallel to the surface. Later, the assertion of Lomas et al. was contradicted. Based on X-ray absorption experiments it was concluded⁵ that benzene adsorbs with the molecular plane parallel to the surface for the low coverage regime there considered (3 L at 80 K). The excitation energies were determined by applied field polarizations. The presence of a π -derived intensity in the σ channel

was attributed to a distortion of the molecular frame rather than to an inclination of the whole ring. Similar conclusions were drawn for benzene on Pt(111).⁶

A density functional theory (DFT) study⁷ using Cu₁₃ cluster models suggested a quinoid structure as the energetically most favored. It was suggested that the adsorption process includes a simultaneous spin-uncoupling in the adsorbate and the substrate, while in the adsorbed molecule an excitation to a triplet state occurs, leading to a rehybridization with an ensuing distortion. The study also found a structure with hydrogen atoms flipped upward, resulting in smaller chemisorption energies. Later,⁸ the involvement of the triplet state in the bonding has been rejected. A theoretical X-ray emission study⁹ in conjunction with NEXAF (Near Edge X-ray Adsorption Fine structure) experimental data predicted the H-flipped geometry as the most favored. There, a Cu₁₃ cluster model was employed for the simulations. Another DFT study⁸ considered the adsorption of benzene in a planar, quinoid and H-flipped shape on different sites in a 2×3 surface

Correspondence to: L. Zotti; e-mail: L.A.Zotti@liverpool.ac.uk

Contract/grant sponsor: EPSRC; contract/grant number: GR/T18592/01, EP/C541898/1

Contract/grant sponsor: European Commission (RADSAS); contract/grant number: NMP3-CT-2004-001561

Contract/grant sponsor: University Research Fellowship of the Royal Society

Table 1. Benzene Adsorption Energies and Relative Geometries.

	3×4		6×6	
	E_{ads} (eV)	Height (\AA) ^a	E_{ads} (eV)	Height (\AA) ^a
A1 top	-0.16	3.20	-0.19	3.13
A2 hollow	-0.26	2.25	-0.45	2.08
A3 [1-10] bridge	-0.33 ^b	2.73 $\theta = 18.46$	-0.28	2.51
A4 [001] bridge	-0.27	2.72	-0.38	2.39
A5 asymmetric	-0.33	2.64 $\theta = 12.91$	-0.42	2.52 $\theta = 10.49$
B1 top	-0.16	3.20	-0.20	3.13
B2 hollow	-0.32	2.38	-0.50	2.17
B3 [1-10]bridge	-0.23	2.81	-0.42 ^c	2.52 $\theta = 14.45$
B4 [001] bridge	-0.25	2.86	-0.33	2.42
B5 asymmetric	-0.35	2.68 $\theta = 13.49$	-0.44	2.43 $\theta = 7.17$

^aHeight of the ring centre with respect to the averaged topmost surface plane. Tilt angles with respect to the surface plane, if larger than 4° , are also reported.

^bShifted to A5.

^cShifted to B5.

supercell. It predicted a range of physisorbed and chemisorbed structures. It was pointed out that a discrimination based solely on the calculated energies was impossible. By analyzing the projected density of states (PDOS) and by comparing the shift in the HOMO orbital energy from the Fermi energy with experimental values, the authors found that the chemisorbed quinoid and H-flipped structures positions are most favored energetically.

Another issue where previous works did not find agreement is the adsorption site. In ref. 10 the adsorption of the isolated benzene molecule on a Cu(110) surface was studied by STM. Here, the molecule and the surface images were scanned at different tunneling conditions. A combination of the two ensuing maps suggested that benzene adsorbs at hollow site. In ref. 11, however, by a similar extrapolation procedure but at different tunneling conditions, a long-bridge site was suggested for the low coverage limit. Long-bridge and hollow sites were also proposed in ref. 8. Moreover, in ref. 10 STM experiments on isolated benzene molecules showed the molecule as a protrusion with a circular shape. This appearance was associated to a flat geometry.

The aim of this work is to clarify the issues and to some extent reconcile existing apparent contradictions. To this end we performed DFT calculations of benzene on Cu(110). For the first time we explicitly show that the preferred adsorption site and geometry depend on the coverage. For a fixed intermolecular distance, we also study the adsorption of fluorobenzene and meta-difluorobenzene on the same Cu(110) surface.

Method

DFT simulations were carried out using the Vienna *ab-initio* Simulation Program (VASP).¹² Exchange and correlation were described by means of the gradient corrected (GGA) PW91 functional.¹³ We used ultrasoft pseudopotentials with a plane wave energy cutoff of 349 eV. The Cu(110) surface was simulated by a four layer slab. Atomic coordinates of the molecule

and the two top copper layers were fully relaxed to 0.01 eV/ \AA . Two different supercells were considered, a 3×4 unit cell (where the longest lattice vector points along $[1\bar{1}0]$) and a 6×6 one. The two supercells correspond to 8.8×10^{13} mol/cm² and 2.9×10^{13} mol/cm² coverage, respectively. Brillouin-zone integrations were carried out sampling on a grid of five special \mathbf{k} -points in the 3×4 unit cell, while in the 6×6 the calculation was limited to the gamma point only. For selected configurations, the molecular charges were calculated within an all-electron scheme, the projected augmented wave (PAW) method.¹⁴ STM simulated images were obtained from the local density distribution, correcting for the effect of high bias values.¹⁵

Results and Discussion

Benzene

In Table 1 we present the data obtained in the two cases. Beside the positions with highest symmetry (top, hollow, and bridge), also one position (A5, B5) with low symmetry was considered (see Fig. 1). In the tables it is labeled as “asymmetric”. In this position, the benzene center lies in the middle between two top atoms in the $[110]$ direction, while in the $[001]$ direction it is distant from the closest row by 1/4 of the $[001]$ Cu—Cu distance. For all positions, two orientations (one rotated by 30° with respect to the other) were considered, the molecule was in all cases positioned parallel to the surface prior to relaxation.

It can be seen that in a 3×4 unit cell the tilted B5 geometry is the most stable, while in a 6×6 this occurs for the flat lying B2 position. The adsorption energy for position A5 is lower than for B5 in both cases by 0.02 eV; in the 3×4 unit cell it is intermediate between B5 and B2. By comparison with a 10 \mathbf{k} -points calculation, the energy difference between B5 and B2 in the 3×4 unit cell was found to be converged within 0.01 eV i.e. by an amount roughly one order of magnitude lower than the absolute change in adsorption energy for B2 (0.18 eV) and B5 (0.09 eV) geometries in the 3×4 and 6×6 unit cells.

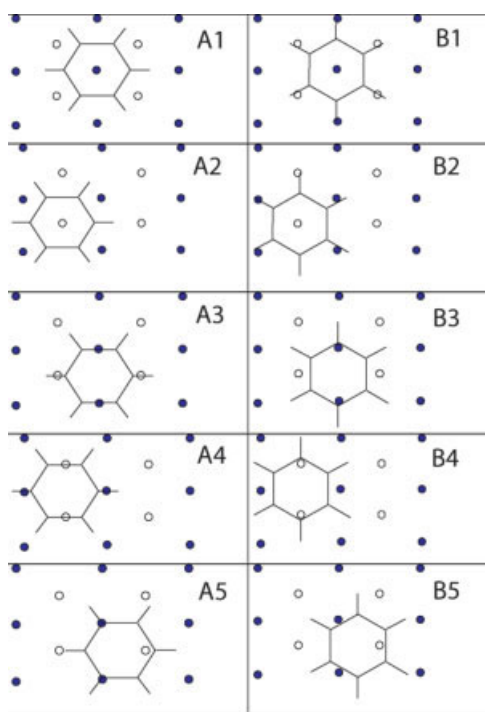


Figure 1. Initial benzene positions. The dark bullets indicate the uppermost atoms. The empty ones indicate the second layer atoms. [Color figure can be viewed in the online issue, which is available at www.interscience.wiley.com.]

Although the absolute values of the calculated adsorption energies results underestimated due to the adopted GGA approximation and the ensuing neglect of dispersion interactions,^{16,17} the basic result which emerges from the calculations i.e. the coverage dependence of both adsorption site and molecular geometry is expected not to be qualitatively affected, as the agreement with experimental data for different coverages further suggests. Furthermore, by leveraging on a thorough report which has recently tested the accuracy of several DFT methods with respect to hydrogen bonding (HB), charge transfer (CT), dipolar interactions (DI), and weak interactions (WI),¹⁷ we also note that, when disregarding HB interactions (which are expected to be negligible for the considered systems), PW91 is reported to perform in a more accurate way than PBE for only CT, DI, and WI interactions (see ref. 17, Table 8) i.e. the three main interactions governing the adsorption of the considered systems. Therefore, in the same spirit of 17 PW91 can be considered as almost competitive (i.e. semi-quantitative) in accuracy to higher level of theory (MP2) but at a much lower computational cost. On these grounds, the adopted XC approximation represents a reasonable trade-off between semi-quantitative accuracy on the one hand and reduced computational cost on the other.

We focused our attention particularly on B2 and B5 configurations, since they are the two most stable adsorption geometries for the considered unit cells i.e. molecular coverage. In positions A5 and B5, the benzene was found tilted with the bottom side near the closest copper row. For the B5 configuration (Fig. 2, right), the hydrogens closer to the surface are bent upwards

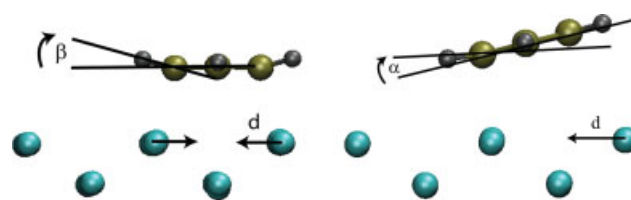


Figure 2. Adsorption induced distortion; d indicates the copper atom displacement, while α and β indicate the hydrogen tilt angles. The picture plane is parallel to the [001] direction. Left: B2 position. For 3×4 unit cell: $\beta = 7.1^\circ$, $d = 0.03 \text{ \AA}$; for 6×6 : $\beta = 13.4^\circ$, $d = 0.05 \text{ \AA}$. Right: B5 position. For 3×4 unit cell: $\alpha = 6.8^\circ$, $d = 0.005 \text{ \AA}$; for 6×6 : $\alpha = 8.3^\circ$, $d = 0.016 \text{ \AA}$. [Color figure can be viewed in the online issue, which is available at www.interscience.wiley.com.]

(6.8° in 3×4 unit cell and 8.3° in 6×6). A similar deformation (5.7°) has been found in the A5 configuration. Interestingly, when no molecular symmetry constraint is enforced in the simulation (at odds with ref. 7), for some short-bridge adsorption sites the benzene is modeled to shift to A5 (B5) positions upon optimization.

In B2 four C—H bonds are on top of copper atoms, while the other two bonds are between copper $[1\bar{1}0]$ rows (see Fig. 1). In the 6×6 unit cell the hydrogen atoms closer to Cu are tilted by 13.4° , while other two are tilted by 6° (Fig. 2, left). The resulting structure looks very similar to the H-flipped one found by Triguero in ref. 7. The distortion was found to be less pronounced in the 3×4 unit cell: the hydrogens close to Cu are tilted by 7.1° , while the other two are tilted by 3.8° . Moreover, the carbon ring in 4×3 is 0.21 \AA farther from the surface than in 6×6 . Hydrogen bending is also seen in the A2 position in a 3×4 (9°) and 6×6 (14.2°) unit cell. These deformations indicate an $sp^2 \rightarrow sp^3$ rehybridization for the benzene carbon atoms whenever they come close to the surface atoms, as suggested in ref. 7 for the hollow position.

Beside the benzene structure distortion, a rearrangement in the copper substrate also occurs. In Figure 2 the displacement of the copper atoms in $[1\bar{1}0]$ rows in the B2 configuration is indicated by arrows. The copper atoms closer to the benzene, move towards the benzene ring by 0.05 \AA in the 6×6 unit cell, while they move by 0.03 \AA in the 3×4 unit cell. In the direction normal to the surface, they shift upwards in both cases, but are 0.02 \AA higher in a 6×6 than in a 3×4 unit cell. The overall rearrangement reduces the Cu—C distance from $2.48\text{--}2.49 \text{ \AA}$ for the 3×4 unit cell to $2.26\text{--}2.27 \text{ \AA}$ in the 6×6 unit cell.

Table 2. Surface Strain.

	Coupled system	Molecule	Surface	Strain
B2-4×3	−234.75	−76.19	−158.09	0.47
B5-4×3	−234.78	−76.25	−158.10	0.42
B2-6×6	−548.83	−75.97	−471.86	1.00
B5-6×6	−548.78	−76.21	−471.91	0.66

All the energy values are given in eV.



Figure 3. Electronic charge accumulation for B5 position along the [001] direction in a 3×4 unit cell (left) and in a 6×6 (right). The visualized isosurface value is $2.5 \times 10^{-6} \text{ e}\text{\AA}^{-3}$ and $8.2 \times 10^{-7} \text{ e}\text{\AA}^{-3}$, respectively. In the 3×4 unit cell the bonding occurs exclusively between the two closest copper atoms and the lowest carbon atoms. In a 6×6 the bonding involves both sides of the benzene ring. Consequently the tilt angle decreases.

To quantify the energetics of the surface rearrangements we calculated the surface strain. It was evaluated as the difference between the energy of the coupled system and the energy of isolated slab and molecule in the adsorption induced geometry. The calculated values are listed in Table 2.

It turns out that the strain is significantly larger for the 6×6 unit cell, which indicates the rearrangements is more restricted in a 3×4 unit cell than in a 6×6 .

What makes one position more stable than another is how much the orbitals overlap between copper and carbon atoms. While the B2 position requires a sufficient surface strain along two sides of the benzene to create the best conditions for the bonding, the position B5 mainly involves only one couple of carbon atoms. Since in a 3×4 unit cell a large surface strain is not possible, the B5 position is preferred. In a 6×6 unit cell, instead, the surface strain allows the benzene to relax into a hollow position and, since this position involves more channels (in space) for charge transfer, the adsorption energy increases.

This can also be seen from the bond lengths between carbon atoms and the closest copper atoms, if we consider that shorter bond lengths correspond to stronger bonds. The bond length for Cu–C in a 3×4 unit cell is 2.42 Å for the B5 configuration, while is 2.48–2.49 Å for the B2 one. In a 6×6 unit cell, instead, the bond length is 2.30 Å for B5, while it is 2.26–2.27 Å for B2.

In Figures 3 and 4 the charge transfer for both configurations is reported. It was evaluated as the charge difference between the coupled system and the isolated slab and molecule in the adsorption induced geometry. This kind of analysis is particularly well suited to describe localization in real space of metal-



Figure 4. Electronic charge accumulation for B2 position along the [001] direction in a 3×4 unit cell (left) and in a 6×6 (right). It can be observed how in the 6×6 the charge overlap between benzene and copper increases.

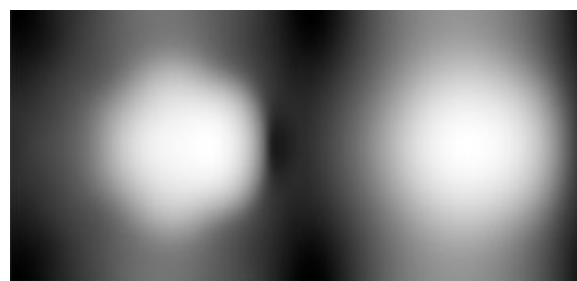


Figure 5. Simulated STM images for benzene in the B5 position in a 3×4 unit cell. Sample voltage = -0.1V . Left: at about 3 Å. Right: at about 5 Å.

molecule bonding. They explain why in the B5 position the benzene is less tilted in a 6×6 unit cell than in a 3×4 . The reason is that, in a 6×6 unit cell, the benzene starts bonding with copper atoms also on the other side, experiencing therefore an attractive interaction. This additional bonding is now possible (while it was not in 3×4 unit cell) because the copper atoms can rearrange here more easily. The charge plots also show how, for the B2 configuration, the charge overlap between copper and benzene increases going from the 3×4 unit cell to the 6×6 .

A detailed investigation on the distance by which one position starts to be preferred to another is not possible at the moment. This is because experimental information about the exact adlayer geometry is not available and searching for it is computationally too demanding (here it has been assumed that the unit cell is rectangular, but also other unit cells may result). However, what is relevant is that we obtain different results for two different intermolecular distances; hence, a note of caution is in place with respect to the unit cell size if one wants to study this kind of system as isolated. Since the differences in adsorption energies are rather small, it cannot be excluded that thermal fluctuations may lead to both, tilted and flat geometries, in the same adlayer. The main conclusion is that the possibility of tilting cannot be excluded, especially for molecular coverage higher than $8.8 \times 10^{13} \text{ mol/cm}^2$ corresponding to a 3×4 unit cell.

Since it turns out that the final adsorption for benzene on Cu(110) stems from a delicate balance between surface relaxa-

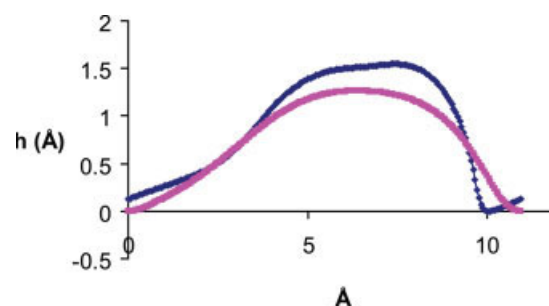


Figure 6. Scanline reporting the apparent corrugation (h) for the images of Figure 5 along the horizontal direction (001), passing through the highest point. Blue and red lines correspond to left and right image, respectively.

Table 3. Relative Adsorption Energies for Fluorobenzene (the Zero Has Been Assigned to the Lowest Adsorption Energy (−0.24 eV).

Geometry	E_{ads} (meV)	Θ^a	Geometry	E_{ads} (meV)	Θ
A1x	143	Horizontal	B1x	152	Horizontal
A1y	138	8.0 ^b	B1y	146	Horizontal
A2x	113	Horizontal	B2x	82	Horizontal
A2y	89	Horizontal	B2y	84	5.9 ^c
A3x	92	Horizontal	B3x	119	5.1 ^d
A3y	104	7.3 ^c	B3y	105	Horizontal
A4x	117	Horizontal	B4x	99	Horizontal
A4y	88	Horizontal	B4y	100	5.9 ^c
A5x	19	15.8 ^b	B5x	34	18.8 ^b
A5x*	95	8.8 ^b	B5x*	Equivalent to B5x	
A5y	0	16.5 ^b	B5y	1	16.1 ^b
A5y*	108	13.5 ^c	B5y*	112	7.3 ^c

The positions signed with an asterisk (*) are reflected with respect to the [1-10] direction.

^aFluorobenzene benzene ring dihedral angle with respect to the surface. Angles less than 4° are approximated to horizontal orientation.

^bRotated around [001] axis.

^cRotated around [1-10] axis.

^dRotated around an axis with components on both [001] and [1-10] axis.

tion on one hand and molecular distortion on the other, the presented result in our view provide valuable insights over previous 2×3 unit cell calculations with frozen layers,⁸ and symmetry constrained⁷ data.

Finally, we performed STM simulations to study the appearance of tilted benzene like in the B5 position (in a 3×4 unit cell). A sample voltage of −0.1 V as in ref. 11 was chosen. In Figure 5 the ensuing simulated images at two different distances from the molecule are shown. It can be observed that the asymmetry in the (001) direction is highly visible only at very close distances from the surface. In Figure 6 we report a scanline along the same direction. The image becomes much more symmetric, as the distance increases.

This indicates that STM can provide information about the benzene adsorption geometry only at short tip-surface distance.

Fluorobenzene and Difluorobenzene

To study the adsorption of fluorobenzene and difluorobenzene on Cu(110) we limited our calculations to the 3×4 unit cell, since studying all the possible configurations in a 6×6 unit cell is too demanding. Here, the top three Cu layers were relaxed. Although not fully quantitative, on the basis of the result of Zhao et al.¹⁷ it is possible to speculate that the accuracy of the adopted GGA approximation is expected to be a reasonable trade-off between semi-quantitative accuracy on the one hand and computational cost on the other also for the fluorine-based compounds here considered. The adsorption of fluorobenzene on Cu(110) has been already studied in ref. 18 by DFT, using a linear combination of atomic orbital (LCAO) implemented in the CRYSTAL98 package. A supercell was used, which allows an intermolecular separation of about 5 Å. There,

a bridging position in the [001] direction was predicted to be the most stable. It was assumed, though, that the adsorption of fluorobenzene occurs at sites of maximum symmetry. In this work, as in the case of benzene, also a lower symmetry position (A5, B5) has been considered. In Table 3 the calculated adsorption energies for all configurations are reported. In Figure 7 the convention for assigning x or y index to different orientations is shown. (For the explicit graphical representation of all the positions see additional materials). Since the number of configurations is double with respect to the simple benzene case, the adsorption energies are expressed relative to the lowest value (i.e. most stable position), for a more concise presentation.

It can be seen that the most stable positions are the ones where the fluorine is connected to the carbon atoms farther away from the surface (A5x, A5y, B5y). For a given geometry, the fluorine position also seems to affect the dihedral angle of the benzene ring with respect to the surface. The ring rotates upwards to position the fluorine atom far from the surface. In Figure 8 it is shown how the tilt angle of the B5 configuration changes according the carbon atom connected to fluorine. Generally, this behavior can be reconciled with the well-known polarophobic nature of the C—F bond,¹⁹ which increases the distance from induced dipoles and charge transfers. Also, the fluorine electronegativity seems to affect the charge transfer from the molecule to the surface. An electron charge loss of 0.106 e was evaluated for the benzene molecule in B5 position, while for the fluorobenzene in the B5y* and B5y the value was found to be 0.055 e and 0.097e, respectively. The charges were calculated within Wigner Seitz radius spheres around each ion. It turns out that fluorine, close to the surface, decreases the stability of the

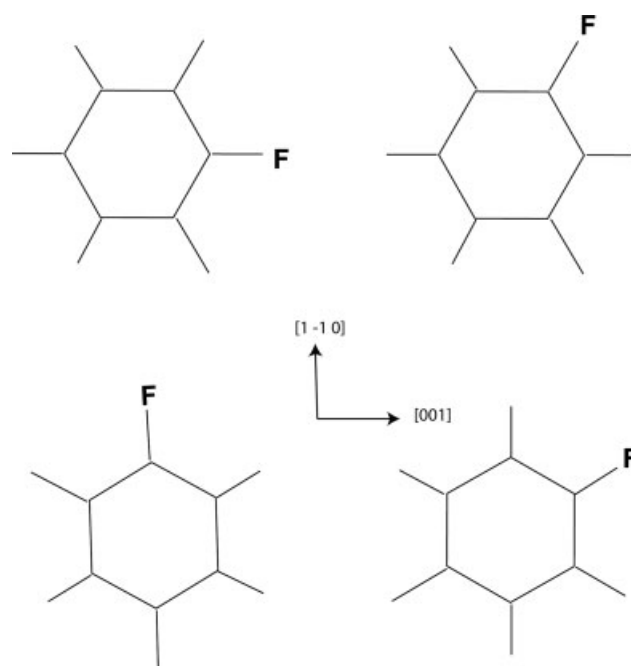


Figure 7. Fluorobenzene orientations: Ax (top left), Ay (top right), Bx (bottom left), By (bottom right). For each of them, the 1-5 previous positions (see Fig. 1) have been considered.

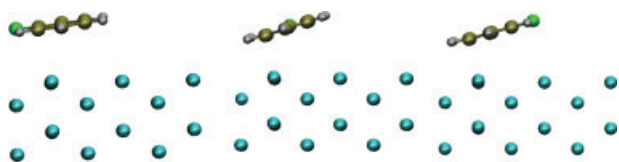


Figure 8. Optimized structure for fluorobenzene in positions (from left) B5y* (7.3°), B5x (18.8°), B5y (16.1°). The fluorine is in green. The picture plane is parallel to the [001] direction.

system, because it hinders the transfer of charge from the molecule. This aspect is confirmed by a Bader²⁰ charge analysis (not shown). However, the presence also of a back donation process from the surface to the molecules is revealed by slight charge losses (0.003 e) of copper atoms in close proximity to carbon atoms. This would confirm the model proposed by Chatt and Duncanson²¹ for aromatic molecules, where donation from the π orbitals of the molecule to the metal and back-donation to molecular antibonding orbitals are both considered. A chemisorption weakening induced by the fluorine was already pointed out in ref. 18 for the fluorobenzene adsorbed in a flat bridging position.

To study the adsorption of difluorobenzene on Cu(110), we first compared the energy of the three possible kinds of difluorobenzene in the gas phase: 1,4-difluorobenzene (*para*), 1,3-difluorobenzene (*meta*) and 1,2-difluorobenzene (*ortho*).

Meta-difluorobenzene was found to be more stable by 0.041 eV than paradifluorobenzene and by 0.166 eV compared to ortho-difluorobenzene. These data are in good agreement with DFT studies performed with Gaussian 94²² at the B3LYP/6-

Table 4. Relative Adsorption energies for meta-di-fluorobenzene (the zero has been assigned to the lowest adsorption energy (-0.17 eV)).

Geometry	E_{ads} (meV)	Θ°	Geometry	E_{ads} (meV)	Θ°
A1x	92	6.1 ^a	B1x	105	Horizontal
A1y	93	9.8 ^a	B1y	109	Horizontal
A2x	78	Horizontal	B2x	91	5.0 ^d
A2y	76	Horizontal	B2y	78	4.6 ^a
A3x	66	7.8 ^b	B3x	80	Horizontal
A3y	0 ^c	21.8 ^a	B3y	71	8.5 ^d
A4x	88	6.7 ^a	B4x	88	6.3 ^d
A4y	70	Horizontal	B4y	74	4.5 ^b
A5x	92	8.6 ^b	B5x	83	6.1 ^b
A5y	7	12.1 ^a	B5y	21	14.1 ^b
A5x*	62	Horizontal	B5x*	Equiv. to B5x	
A5y*	123	Horizontal	B5y*	88	Horizontal

The positions signed with an asterisk (*) are reflected with respect the [1-1 0] direction^c

^aRotated around [1-10] axis.

^bRotated around an axis with components on both [001] and [1-10] axis.

^cShifted to A5y.

^dRotated around [001] axis.

^eDifluorobenzene ring dihedral angle with respect to the surface. Angle less than 4° are approximated to horizontal orientation.

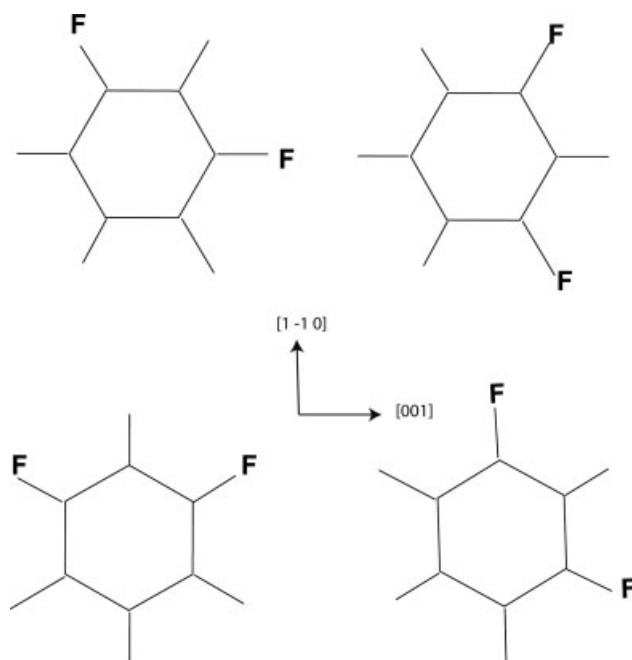


Figure 9. Meta-di-fluorobenzene orientations: Ax (top left), Ay (top right), Bx (bottom left), By (bottom right). For each of them, 1-5 previous positions (see Fig. 1) have been considered.

311G* level²³. Accordingly, we decided to study only the adsorption of metadifluorobenzene on Cu(110). In Table 4 we report the adsorption energies. The conclusions are very similar to the case of fluorobenzene: the lowest adsorption energies are found for the A5y position (see Figs. 9 and 10), where both fluorine atoms are far from the surface and the rotation around the [1 $\bar{1}$ 0] axis is possible.

Finally, we performed STM simulation on the fluorobenzene at the same bias voltage as for the benzene, to study how the benzene appearance is modified by the presence of fluorine. In Figure 11 the ensuing images are shown for the B5y configura-

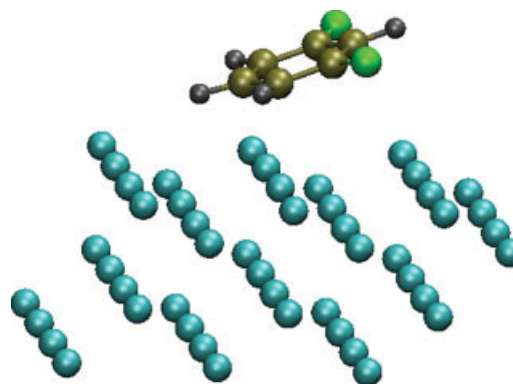


Figure 10. Meta-di-fluorobenzene in the most stable positions (A5y). Fluorine atoms are in green.

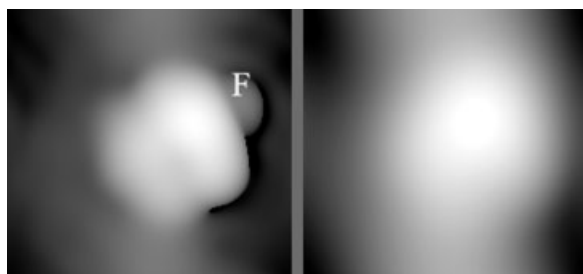


Figure 11. Simulated STM images for fluorobenzene in the B5y position in a 3×4 unit cell. Sample voltage = -0.1 V. Left: at about 2.5 \AA . Right: at about 5 \AA .

tion. The fluorine is visible only at short distance from the surface (2.5 \AA), while it disappears as the distance increases. Generally the image is dominated by the π -system. The highest intensity spot corresponds to the highest carbon atom (i.e. the one connected to the fluorine), but its identification would require a very high tip resolution. Very similar conclusions were drawn by performing a simulation at $+0.3 \text{ V}$ and -2 V (not shown). In ref. 18 STM simulations at 2.5 \AA from the surface were performed. There, very few topographical differences between the benzene and fluorobenzene images were found. In our case, the same conclusion can be drawn at larger distances from the surface, where the benzene and fluorobenzene appearance appear quite similar and no significant variations in the contrast is found.

Conclusions

The adsorption of benzene, fluorobenzene and metadifluorobenzene on Cu(110) has been studied by DFT. For the benzene, two different unit cells were considered. At high coverage a tilted geometry results to be the most stable, while at low coverage a slightly deformed horizontal geometry is preferred. The reason is attributed to a different strain induced in the substrate. For fluorobenzene and metadifluorobenzene, the same positions as for the benzene result to be favored. The dihedral angle and the adsorption energy value result to be affected by the position of the fluorine atoms. It turns out that in the most stable configurations the fluorine is far from the surface. STM simulations revealed that the fluorine can be identified only at close distances from the surface.

References

1. Tour, J. M.; Jones, L., II; Pearson, D. L.; Lamba, J. J. S.; Burgin, T. P.; Whitesides, G. M.; Allara, D. L.; Parikh, A. N.; Altre, S. V. *J Am Chem Soc* 1995, 117, 9529.
2. Foster, A.; Hofer, W. A. *Scanning Probe Microscopy*, Springer: New York, 2006; Chapter 7.
3. Wang, L.; Liu, L.; Chen, W.; Feng, Y.; Wee, A. T. S. *J Am Chem Soc* 2006, 128, 8003.
4. Lomas, J. R.; Baddeley, C. J.; Tikhov, M. S.; Lambert, R. M. *Chem Phys Lett* 1996, 263, 591.
5. Weinelt, M.; Wassdahl, N.; Wiell, T.; Karis, O.; Hasselstrom, J.; Bennich, P.; Nilsson, A.; Stohr, J.; Samant, M. *Phys Rev B* 1998, 58, 7351.
6. Mainka, C.; Bagus, P. S.; Schertel, A.; Strunskus, T.; Grunze, M.; Wöll, Ch. *Surf Sci* 1995, 341, L1055.
7. Triguero, L.; Pettersson, L. G. M.; Minaev, B.; Agren, H. *J Chem Phys* 1998, 108, 1193.
8. Bilic, A.; Reimers, J. R.; Hush, N. S.; Hoft, R. C.; Ford, M. J. *J Chem Theory Comp* 2006, 2, 1093.
9. Peterson, L. G. M.; Agren, H.; Luo, Y.; Triguero, L. *Surf Sci* 1998, 408, 1.
10. Komeda, T.; Kim, Y.; Fujita, Y.; Sainoo, Y.; Kawai, M. *J Chem Phys* 2004, 120, 5347.
11. Doering, M.; Rust, H.-P.; Briner, B. G.; Bradshaw, A. M. *Surf Sci Lett* 1998, 410, L736.
12. (a) Kresse, G.; Hafner, J. *Phys Rev B* 1993, 47, 558; (b) Kresse, G.; Furthmüller, J.; *Phys Rev B* 1996, 54, 11169.
13. Perdew, J. P.; Chevary, J. A.; Vosko, S. H.; Jackson, K. A.; Pederson, M. R.; Singh, D. J.; Jiolhais, C. *Phys Rev B* 1992, 46, 6671.
14. Blochl P. E. *Phys Rev B* 1994, 50, 17953.
15. Palotas, K.; Hofer, W. A. *J Phys Condens Mater* 2005, 17, 2705.
16. Ortmann, F.; Bechstedt, F. *Phys Rev B* 2006, 73, 205101/1–10.
17. Zhao, Y.; Truhlar, D. G. *J Chem Theory Comput* 2005, 1, 415.
18. Rogers, B. L.; Shapter J. G.; Ford, M. J. *Model Simul Mater Sci Eng* 2004, 12, 1109.
19. Graham Solomones T. W. *Organic Chemistry*, Wiley: New York, 1996; Chapter 2.
20. Henkelman, G.; Arnaldsson, A.; Jonsson, H. *Comp Mater Sci* 2006, 36, 354.
21. Chatt, J.; Duncanson, L. A. *J Chem Soc* 1953, 77, 2939.
22. Gaussian 03, Revision C.02, Frisch, M. J.; Trucks, G. W.; Schlegel, H. B.; Scuseria, G. E.; Robb, M. A.; Cheeseman, J. R.; Montgomery, J. A., Jr.; Vreven, T.; Kudin, K. N.; Burant, J. C.; Millam, J. M.; Iyengar, S. S.; Tomasi, J.; Barone, V.; Mennucci, B.; Cossi, M.; Scalmani, G.; Rega, N.; Petersson, G. A.; Nakatsuji, H.; Hada, M.; Ehara, M.; Toyota, K.; Fukuda, R.; Hasegawa, J.; Ishida, M.; Nakajima, T.; Honda, Y.; Kitao, O.; Nakai, H.; Klene, M.; Li, X.; Knox, J. E.; Hratchian, H. P.; Cross, J. B.; Bakken, V.; Adamo, C.; Jaramillo, J.; Gomperts, R.; Stratmann, R. E.; Yazyev, O.; Austin, A. J.; Cammi, R.; Pomelli, C.; Ochterski, J. W.; Ayala, P. Y.; Morokuma, K.; Voth, G. A.; Salvador, P.; Dannenberg, J. J.; Zakrzewski, V. G.; Dapprich, S.; Daniels, A. D.; Strain, M. C.; Farkas, O.; Malick, D. K.; Rabuck, A. D.; Raghavachari, K.; Foresman, J. B.; Ortiz, J. V.; Cui, Q.; Baboul, A. G.; Clifford, S.; Cioslowski, J.; Stefanov, B. B.; Liu, G.; Liashenko, A.; Piskorz, P.; Komaromi, I.; Martin, R. L.; Fox, D. J.; Keith, T.; Al-Laham, M. A.; Peng, C. Y.; Nanayakkara, A.; Challacombe, M.; Gill, P. M. W.; Johnson, B.; Chen, W.; Wong, M. W.; Gonzalez, C.; and Pople, J. A.; Gaussian, Inc., Wallingford CT, 2004.
23. Taskinen, E. *Struct Chem* 2000, 11, 293.